





Rifabutin Is Bactericidal against Intracellular and Extracellular Forms of *Mycobacterium abscessus*

 Matt D. Johansen,^a Wassim Daher,^{a,b} Françoise Roquet-Banères,^a Clément Raynaud,^a Matthéo Alcaraz,^a
 Florian P. Maurer,^{c,d}  Laurent Kremer^{a,b}

^aCentre National de la Recherche Scientifique UMR 9004, Institut de Recherche en Infectiologie de Montpellier (IRIM), Université de Montpellier, Montpellier, France

^bINSERM, IRIM, Montpellier, France

^cNational and WHO Supranational Reference Center for Mycobacteria, Research Center Borstel-Leibniz Lung Center, Borstel, Germany

^dInstitute of Medical Microbiology, Virology, and Hygiene, University Medical Center Hamburg-Eppendorf, Hamburg, Germany

ABSTRACT *Mycobacterium abscessus* is increasingly recognized as an emerging opportunistic pathogen causing severe lung diseases. As it is intrinsically resistant to most conventional antibiotics, there is an unmet medical need for effective treatments. Repurposing of clinically validated pharmaceuticals represents an attractive option for the development of chemotherapeutic alternatives against *M. abscessus* infections. In this context, rifabutin (RFB) has been shown to be active against *M. abscessus* and has raised renewed interest in using rifamycins for the treatment of *M. abscessus* pulmonary diseases. Here, we compared the *in vitro* and *in vivo* activity of RFB against the smooth and rough variants of *M. abscessus*, differing in their susceptibility profiles to several drugs and physiopathological characteristics. While the activity of RFB is greater against rough strains than in smooth strains *in vitro*, suggesting a role of the glycopeptidolipid layer in susceptibility to RFB, both variants were equally susceptible to RFB inside human macrophages. RFB treatment also led to a reduction in the number and size of intracellular and extracellular mycobacterial cords. Furthermore, RFB was highly effective in a zebrafish model of infection and protected the infected larvae from *M. abscessus*-induced killing. This was corroborated by a significant reduction in the overall bacterial burden, as well as decreased numbers of abscesses and cords, two major pathophysiological traits in infected zebrafish. This study indicates that RFB is active against *M. abscessus* both *in vitro* and *in vivo*, further supporting its potential usefulness as part of combination regimens targeting this difficult-to-treat mycobacterium.

KEYWORDS *Mycobacterium abscessus*, rifabutin, macrophage, zebrafish, therapeutic activity

Nontuberculous mycobacteria (NTM) are environmental mycobacteria. Among all NTM, *Mycobacterium avium* and *Mycobacterium abscessus* represent the most frequent pathogens associated with pulmonary disease (1). *M. abscessus* is a rapidly growing NTM of increasing clinical significance, particularly in cystic fibrosis (CF) patients (2). In CF patients, infection with *M. abscessus* correlates with a more rapid decline in lung function and can represent an obstacle to subsequent lung transplantation (3–5). From a taxonomical view, the species currently comprises three subspecies, *M. abscessus* subsp. *abscessus* (here designated *M. abscessus*), *M. abscessus* subsp. *bolletii* (here designated *M. bolletii*), and *M. abscessus* subsp. *massiliense* (here designated *M. massiliense*) (6). These subspecies exhibit different clinical outcomes and drug susceptibility profiles to antibiotic treatments (7).

M. abscessus strains can exhibit either a smooth (S) or rough (R) morphotype as a consequence of the presence or absence, respectively, of bacterial surface glycopep-

Citation Johansen MD, Daher W, Roquet-Banères F, Raynaud C, Alcaraz M, Maurer FP, Kremer L. 2020. Rifabutin Is bactericidal against intracellular and extracellular forms of *Mycobacterium abscessus*. *Antimicrob Agents Chemother* 64:e00363-20. <https://doi.org/10.1128/AAC.00363-20>.

Copyright © 2020 American Society for Microbiology. All Rights Reserved.

Address correspondence to Laurent Kremer, laurent.kremer@irim.cnrs.fr.

Received 25 February 2020

Returned for modification 4 May 2020

Accepted 3 August 2020

Accepted manuscript posted online 17 August 2020

Published 20 October 2020

tidolipids (GPL) (1, 8–10). These morphological distinctions are associated with important physiological differences. S variants are more hydrophilic than R variants, enabling increased sliding motility and the capacity to form biofilms (8, 9, 11), while the aggregative R variants possess a high propensity to produce large bacterial cords (11, 12). While S and R variants can be viewed as two representatives of the same isolate, which can coexist and evolve differently in response to host immunity, they express different pathophysiological traits (10). S variants are typically less virulent than the R variants (11, 13, 14), the latter being more frequently associated with severe lung diseases and persisting for years in CF patients (3, 5). Importantly, an S-to-R transition within the colonized host (5, 15) is linked to genetic polymorphisms within the GPL biosynthetic/transport locus (15, 16). Moreover, differences in the susceptibility to drug candidates have been identified between S and R variants (17, 18), highlighting the need for the improved evaluation of new compounds/drug regimens against both morphotypes.

Treatment of *M. abscessus* lung disease remains particularly challenging, largely due to intrinsic resistance to a wide panel of antimicrobial agents, including most antitubercular drugs such as rifampin (RIF) (19–22). The extensive resistome of *M. abscessus* results from a low permeability of the cell wall, absence of drug-activating systems, induction of efflux pumps, and production of a wide panel of drug-modifying enzymes (19, 22, 23). In addition, mutations in genes encoding drug targets can result in acquired drug resistance, further complicating therapy (1, 24). Treatment of infections caused by *M. abscessus* require prolonged courses of multiple antibiotics, usually combining a macrolide (azithromycin or clarithromycin), a β -lactam (imipenem or ceftazidime), and an aminoglycoside (amikacin) (25–27). Additional drugs, such as tigecycline or clofazimine, are often added to strengthen the regimen, particularly in response to toxic side effects or unsatisfactory clinical response (28). Despite intensive chemotherapy, treatment success rates typically remain around 25 to 40% in the case of macrolide resistance, which occurs in at least 40 to 60% of clinical isolates (29). Therefore, there is an urgent clinical need for new drug regimens with improved efficacy (30). While the current drug pipeline against *M. abscessus* remains poor, it has recently been fueled with the discovery of several active hits and the development of repurposed drugs (24). Among the latter, screening of libraries of approved pharmaceuticals revealed that rifabutin (RFB), a rifamycin related to the poorly active rifampicin (RIF), shows activity against *M. abscessus* (31, 32). RIF, along with many other rifamycins, is inactivated by the ADP-ribosyltransferase (Arr_{Mab}) encoded by *MAB_0591*, which ribosylates the drug at the C23 hydroxyl position (33). RFB has also been reported to be as active as clarithromycin in immunocompromised NOD/SCID mice infected with *M. abscessus* (34). However, most studies of RFB have been carried out on either S or R variants (when reported), rendering results sometimes difficult to interpret and/or to compare. Due to the coexistence of S and R variants in patients (15) and the presence of each variant in different compartments (S residing mostly in macrophages and R growing also in the form of intra- or extracellular cords), it is essential to address the activity of RFB on isogenic S/R pairs in both *in vitro* and *in vivo* studies.

The present study aimed to describe and compare the activity of RFB against S and R *M. abscessus* complex strains *in vitro* and *ex vivo* in a macrophage infection model. Due to the importance of cording, considered a marker of severity of the infection with the R variant, we also investigated the efficacy of RFB in a zebrafish model of infection.

RESULTS

Rough *M. abscessus* is more susceptible to RFB treatment than smooth *M. abscessus in vitro*. Exposure of exponentially growing *M. abscessus* CIP104536^T S and R isogenic variants to increasing concentrations of RFB, starting at 25 μ g/ml for S and 6.25 μ g/ml for R, resulted in a noticeable growth inhibition (Fig. 1). At the lowest concentration, the CFU at 72 h posttreatment remained comparable to that of the inoculum, suggestive of a bacteriostatic effect. However, the highest RFB concentrations for both S (200 μ g/ml) and R (50 μ g/ml) variants were accompanied by a 1.81- and

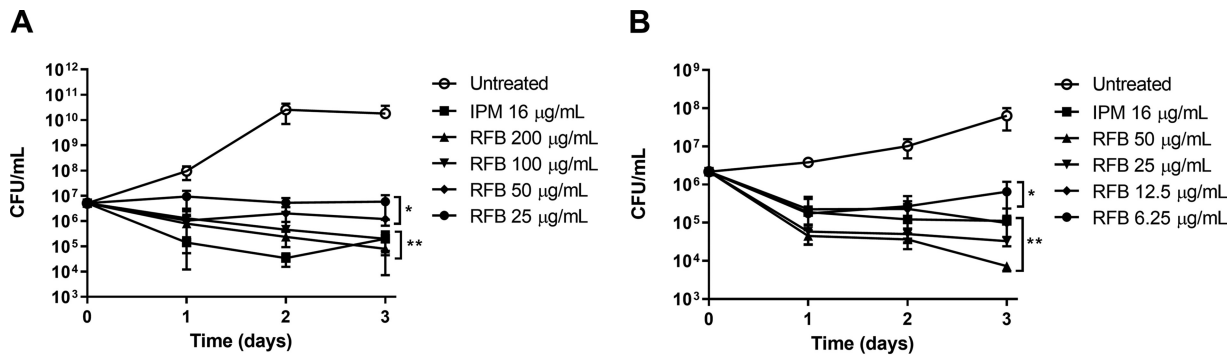


FIG 1 (A and B) *In vitro* activity of rifabutin. *M. abscessus* CIP104536^T S (A) or R (B) was exposed either to 200, 100, 50, 25, 12.5, or 6.25 µg/ml RFB or 16 µg/ml IPM in CaMHB at 30°C. At various time points, bacteria were plated on LB agar and further incubated at 30°C for 4 days prior to CFU counting. Results are expressed as the mean of triplicates ± the standard deviation (SD) and are representative of two independent experiments. *, *P* ≤ 0.05; **, *P* ≤ 0.01.

2.47-log reduction in the CFU counts at 72 h posttreatment, respectively (Fig. 1). While similar bactericidal effects of RFB were observed against both variants, this was achieved with lower concentrations of RFB against the R variant relative to the isogenic S variant. Overall, RFB at concentrations of 12.5 µg/ml (for the R variant) resulted in a killing effect comparable to that of imipenem (IPM) used at the MIC (16 µg/ml), which is known as an active β-lactam drug against *M. abscessus* (35) (Fig. 1).

To confirm the differences in the susceptibility to RFB, we determined the MIC of the CIP104536^T S and R variants in cation-adjusted Mueller-Hinton broth (CaMHB). Table 1 clearly shows that the S strain is 4-fold more resistant than its R counterpart. However, both variants were similarly resistant to other rifamycins (RIF, rifapentine [RPT], and rifaximin [RFX]), in agreement with previous studies (32, 34). Our MIC values, obtained in repetitive experiments with two different commercial sources of RFB, were higher than those reported earlier (32, 34) but comparable to values reported in another study (36). Consistent with other studies (31), we also noticed that the MIC values were dependent on the culture medium (see Table S1 in the supplemental material). Interestingly, MICs of RFB against S and R strains were lower in Middlebrook 7H9 broth than CaMHB, but this effect was lost when supplementing the medium with oleic acid-albumin-dextrose-catalase (OADC) enrichment. In contrast, the S and R strains displayed equal susceptibility levels to RFB in Sauton’s medium.

To investigate the relationship between RFB activity and GPL production, drug susceptibility was assessed in CaMHB using the GPL-deficient $\Delta mmpL4b$ mutant, generated in the S background of the type strain CIP104536^T, and its complemented counterpart (14, 37, 38). The *mmpL4b* gene encodes the MmpL4b transporter, which participates in the translocation of GPL across the inner membrane (37, 39). Mutations in this gene are associated with loss of GPL and acquisition of an R morphotype (13, 37). The parental S strain, and to a lesser extent the $\Delta mmpL4b$ -complemented strain, showed reduced susceptibility to RFB (MIC, 32 to 64 µg/ml) compared to the *M.*

TABLE 1 Drug susceptibility/resistance profile of smooth and rough variants derived from the reference *M. abscessus* 104536^T strain to various rifamycins in CaMHB^a

Strain	Morphotype	MIC (µg/ml) ^a			
		RFB	RIF	RPT	RFX
CIP104536 (S)	S	64	>128	>128	>128
CIP104536 (R)	R	16	>128	>128	>128
Δ MAB_ <i>mmpL4b</i>	R	16	>128	>128	>128
Δ MAB_ <i>mmpL4b</i> _C	S	32	>128	>128	>128
CIP104536 (S) + pMV306-MAB_1409c-HA	S	64	>128	>128	>128
CIP104536 (R) + pMV306-MAB_1409c-HA	R	64	>128	>128	>128

^aMICs (µg/ml) were determined following the CLSI guidelines.

^bRFB, rifabutin; RIF, rifampin; RPT, rifapentine; RFX, rifaximin.

TABLE 2 Comparison of the activity of RFB against clinical isolates from CF and non-CF patients^a

Species and strain	Morphotype	Source	RFB MIC ($\mu\text{g/ml}$)
<i>M. abscessus</i>			
CIP104536	S	Non-CF	50
3321	S	Non-CF	50
1298	S	CF	50
2587	S	CF	100
2069	S	Non-CF	100
CF	S	CF	25
2524	R	CF	25
2648	R	CF	25
3022	R	Non-CF	50
5175	R	CF	25
CIP104536	R	Non-CF	25
<i>M. massiliense</i>			
CIP108297	R	Addison's disease	50
210	R	CF	100
179	R	CF	100
CIP108297	S	Addison's disease	100
140	S	CF	50
185	S	CF	100
107	S	CF	50
122	S	CF	100
120	S	CF	6.25
212	S	CF	100
100	S	CF	100
111	S	CF	100
<i>M. bolletii</i>			
CIP108541	S	None reported	100
114	S	CF	100
17	S	CF	50
116	S	CF	100
97	S	CF	100
112	R	CF	100
19	R	Non-CF	50
10	R	None reported	100
108	R	CF	25

^aThe MIC ($\mu\text{g/ml}$) was determined in cation-adjusted Mueller-Hinton broth for different subspecies belonging to the *M. abscessus* complex. Results are from 3 independent experiments. RFB, rifabutin

abscessus R strain and the GPL-deficient ΔmmpL4b mutant (MIC, 16 $\mu\text{g/ml}$) (Table 1). The MIC results are in agreement with the growth inhibition kinetics (Fig. 1) and suggest that the outer GPL layer influences the activity of RFB.

M. abscessus possesses numerous potential drug efflux systems (39), including MAB_1409c, a homolog of Rv1258c, previously reported to mediate efflux of RIF in *M. tuberculosis* (40). We thus addressed whether overexpression of MAB_1409c induces resistance to RFB in *M. abscessus*. MAB_1409c was cloned in frame with a hemagglutinin (HA) tag in the integrative vector, pMV306. The resulting construct pMV306-MAB_1409c-HA was introduced in both S and R variants, and the expression of MAB_1409c was confirmed by Western blotting analysis using anti-HA antibodies (Fig. S1). Drug susceptibility assessment indicated a 4-fold upshift in the MIC of RFB against the R strain carrying pMV306-MAB_1409c-HA, while no changes in the MIC were observed with the S strain overproducing MAB_1409c (Table 1). This suggests that increasing expression of MAB_1409c in the R variant is likely to mediate efflux of RFB, leading to reduced susceptibility to the drug.

RFB is active against S and R *M. abscessus* isolates *in vitro*. The activity of RFB was next tested using a set of clinical strains isolated from CF patients or non-CF patients. In general, the MIC of R strains were 2 to 4 times lower than those of S strains, although there were variations among the strains (Table 2). Some R strains (10, 112, 179, 210) exhibited higher MIC values (100 $\mu\text{g/ml}$) than the reference CIP104536^T R strain,

TABLE 3 Characteristics of spontaneous RFB-resistant mutants of *M. abscessus*^a

Strain	MIC ($\mu\text{g/ml}$)	Mutation in <i>rpoB</i>	
		SNP	AA change
CIP104536 ^T (R)	12.5		
25.1	50	C1339T	H447Y
25.2	100	C1339G	H447D
50.1	50	C1339T	H447Y
50.2	50	C1355T	S452L

^aMICs ($\mu\text{g/ml}$) were determined in cation-adjusted Mueller-Hinton broth. Resistant strains were derived from the rough *M. abscessus* CIP104536^T parental strain on Middelbrook 7H10 supplemented with either 25 or 50 $\mu\text{g/ml}$ RFB. Single-nucleotide polymorphism identification in *rpoB* (*MAB_3869c*) and corresponding amino acid changes are also indicated. RFB, rifabutin; AA, amino acid.

while one S strain appeared particularly susceptible to RFB (*M. massiliense* 120 with a MIC of 6.25 $\mu\text{g/ml}$). These differences between strains and S/R morphotypes were not observed previously with bedaquiline (BDQ), and S and R variants were also equally sensitive to BDQ (41). Overall, these results demonstrate that RFB is active against *M. abscessus*, including isolates from CF patients, while R variants appear in general more susceptible to RFB than S variants, supporting previous findings (42).

Mutations in *rpoB* confer resistance to RFB. Although rifamycin resistance mechanisms mediated by mutations in the *rpoB* gene coding for the β -subunit of RNA polymerase have been widely described for *M. tuberculosis*, this is not the case for *M. abscessus*. Therefore, to identify the mechanism of resistance of RFB, a genetic approach involving the selection of spontaneous RFB-resistant mutants of *M. abscessus* followed by *rpoB* sequencing was applied. Four spontaneous strains were isolated in the presence of 25 or 50 $\mu\text{g/ml}$ RFB, exhibiting 4- to 8-fold increased resistance levels, respectively, compared to the parental strain (Table 3). Sequencing analyses of *rpoB* identified several single nucleotide polymorphisms (SNPs) across four resistor mutants. In mutants 25.1 and 50.1, a C1339T substitution leading to an amino acid change at position 447 (H447Y) was identified. Similarly, in mutant 25.2, a C1339G replacement was found, resulting in an amino acid substitution at position 447 (H447D). Comparatively, in mutant strain 50.2, another SNP (C1355T) occurred, leading to an amino acid change at position 452 (S452L). A comparison of the growth of different resistant strains on agar plates containing increasing concentrations of RFB is shown in Fig. S2. Whereas RFB abrogated growth of the wild-type S and R strains, growth of all four resistors harboring mutations at either position 447 or 452 sustained bacterial growth at 50 $\mu\text{g/ml}$, confirming that mutations in *rpoB* confer resistance to RFB.

***M. abscessus* S and R strains are equally susceptible to RFB in macrophages.** While RFB has been shown to be active against *M. tuberculosis* in a macrophage infection model (43), this has not been thoroughly investigated for *M. abscessus*. We thus compared the intracellular efficacy of RFB in THP-1 macrophages infected with either S or R variants. First, the cytotoxicity of RFB and RIF against THP-1 cells was investigated over a 3-day exposure period to either drug. Fig. S3 clearly shows that RFB exerts significant cytotoxicity at concentrations of $>25 \mu\text{g/ml}$ and that the kinetics of macrophage killing was more rapid with RFB than with RIF. Based on these results, all subsequent macrophage studies used 50 $\mu\text{g/ml}$ RIF or 12.5 $\mu\text{g/ml}$ RFB. Amikacin (AMK) at 50 $\mu\text{g/ml}$ was added as a positive control. Dimethyl sulfoxide (DMSO)-treated macrophages were included as a negative control for intracellular bacterial replication. At 0, 1, and 3 days postinfection (dpi), macrophages were lysed and plated to determine the intracellular bacterial loads following drug treatment. Whereas the presence of DMSO or RIF failed to inhibit intramacrophage growth of *M. abscessus* S, exposure to RFB strongly decreased the intracellular bacterial loads at 1 dpi, with this effect further exacerbated at 3 dpi (Fig. 2A). As anticipated, treatment with RIF did not show any effect, in agreement with the poor activity of this compound *in vitro* (Table 1). Comparatively, AMK treatment resulted in a significantly reduced intracellular growth rate in both *M. abscessus* S and R variants between 1 and 3 dpi. Interestingly, the RFB

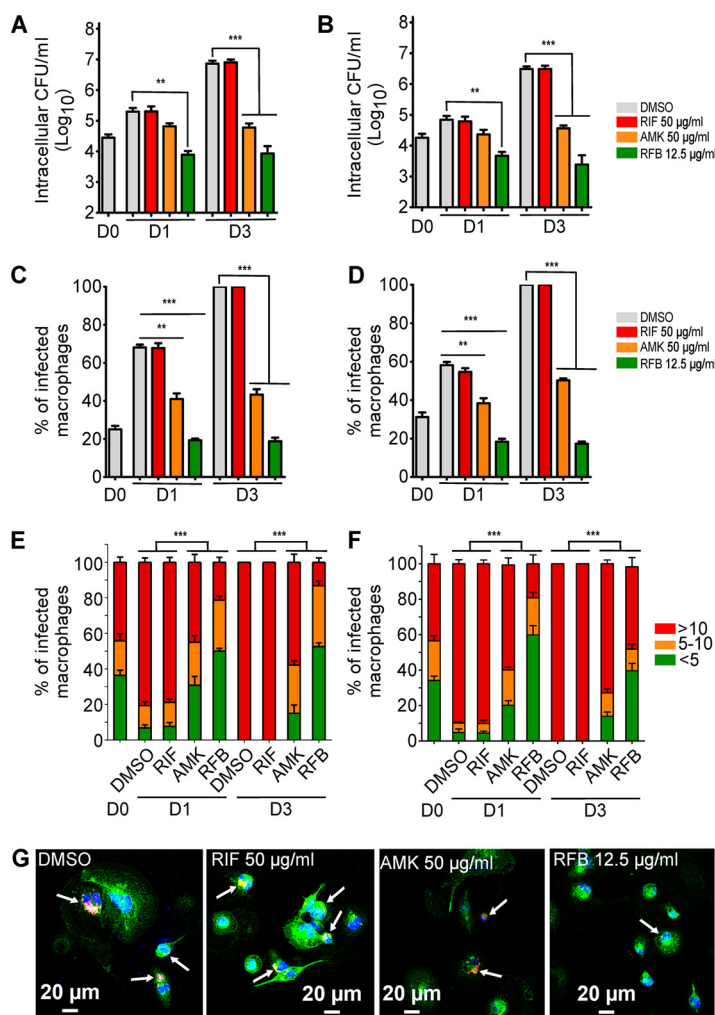


FIG 2 Intracellular activity of RFB on *M. abscessus*-infected THP-1 cells. (A and B) Macrophages were infected with (A) *M. abscessus* S-morphotype and (B) R-morphotype expressing Tdtomato (MOI of 2:1) for 3 h prior to treatment with RIF (50 µg/ml), AMK (50 µg/ml), RFB (12.5 µg/ml), or DMSO. CFU were determined at 0, 1, and 3 dpi. Data are mean values ± SD for three independent experiments. Data were analyzed using a one-way analysis of variance (ANOVA) Kruskal-Wallis test. (C and D) Percentage of infected THP-1 macrophages at 0, 1, and 3 days after infection with (C) *M. abscessus* S or (D) *M. abscessus* R. Data are mean values ± SD for three independent experiments. Data were analyzed using a one-way ANOVA Kruskal-Wallis test. (E) Percentage of S-infected macrophage categories and (F) percentage of R-infected macrophage categories infected with different numbers of bacilli (<5 bacilli, 5 to 10 bacilli, and >10 bacilli). The categories were counted at 0 or at 1 and 3 days postinfection in the absence of antibiotics or in the presence of RIF or AMK at 50 µg/ml or RFB at 12.5 µg/ml. Values are means ± SD from three independent experiments performed in triplicate. (G) Four immunofluorescent fields were taken at 1 day postinfection showing macrophages infected with *M. abscessus* expressing Tdtomato (red). The surface and the endolysosomal system of the macrophages were detected using anti-CD63 antibodies (green). The nuclei were stained with DAPI (blue). White arrows indicate individual or aggregate mycobacteria. Scale bar, 20 µm. **, $P \leq 0.01$; ***, $P \leq 0.001$.

susceptibility profile for the S variant at 1 and 3 dpi was comparable to that of the R variant, with an ~3-log reduction in the CFU counts (Fig. 2A and B, respectively).

Macrophages were next infected with *M. abscessus* strains expressing Tdtomato and exposed to either DMSO, AMK, RIF, or RFB, followed by staining with anti-CD63 and DAPI (4',6-diamidino-2-phenylindole) and observation under a confocal microscope. A quantitative analysis confirmed the marked reduction in the number of *M. abscessus* S-infected THP-1 cells treated with AMK and RFB at 1 and 3 dpi compared to RIF-treated cells or untreated control cells (Fig. 2C). A similar trend was observed when macrophages were infected with *M. abscessus* R (Fig. 2D).

Macrophages infected with the S variant were then classified into three categories based on their bacterial burden, poorly infected (<5 bacilli), moderately infected (5 to 10 bacilli), and heavily infected (>10 bacilli) macrophages. Cells containing bacilli were then individually observed under the microscope and scored to one of the three categories. The quantitative analysis indicates that exposure to RFB significantly reduces the percentage of S variant heavily infected THP-1 cells while increasing the proportion of the poorly infected category compared to the untreated cells at 1 dpi (Fig. 2E). At 3 dpi, the effect of RFB was even more pronounced, with 10% of the infected bacilli belonging to the heavily infected category and more than 50% associated with the poorly infected category. Analysis performed on cells infected with the R variant generated a similar category profile, although treatment with RFB was associated with a higher proportion of heavily infected macrophages at 3 dpi with the R variant than with the S variant (Fig. 2F). Fig. 2G illustrates the reduced number of *M. abscessus* S in infected THP-1 cells treated with RFB at 1 dpi compared to the untreated control cells (DMSO) or those treated with RIF or AMK. Collectively, these results indicate that RFB enters THP-1 macrophages and similarly impedes bacterial replication of both *M. abscessus* S and R variants.

RFB reduces the intramacrophage growth of clinical isolates. RFB has recently shown vast potential as an effective antibiotic for the treatment of *M. abscessus* infection in a NOD/SCID murine model (34). However, to date, the efficacy of RFB has only been evaluated against a limited panel of *M. abscessus* clinical isolates within an infection setting. As such, we explored the activity of RFB against S and R clinical isolates of the *M. abscessus* complex with varying MIC values against RFB within THP-1 macrophages. In support of our previous findings in infected macrophages, RFB treatment (12.5 or 25 $\mu\text{g/ml}$) was very active against all *M. abscessus* subspecies within macrophages at 1 and 3 dpi compared to day 0 and DMSO treatment (Fig. 3), irrespective of S and R morphotypes and the corresponding MIC values (Table 2). Overall, these findings suggest that RFB is very effective against intracellular clinical isolates and highlights the lack of direct correlation between MICs determined *in vitro* and the intracellular activity of RFB.

Reduced intra- and extracellular cording by RFB treatment. An important phenotypic difference between S and R morphotypes is that R morphotypes display increased bacterial aggregation. R bacilli remain attached during replication, forming compact colonies containing structures that resemble cords on agar and in broth medium (8, 12, 14). Fig. 4A clearly shows that, upon infection with *M. abscessus* R expressing TdTomato, the total number of cords per field was significantly reduced in the presence of 50 $\mu\text{g/ml}$ AMK or 12.5 $\mu\text{g/ml}$ RFB compared to 50 $\mu\text{g/ml}$ RIF or DMSO alone. Moreover, we observed intracellular cords that are capable of growing inside the macrophage as well as in the extracellular milieu, which were easily observable at 3 dpi (Fig. 4B). As illustrated in Fig. 4C, treatment with AMK or RFB strongly impacted both intra- and extracellular cords. While AMK treatment severely reduced the number of both intra- and extracellular cords, this effect was almost completely abrogated with RFB at 3 dpi. Together, these results indicate that RFB is highly effective in reducing *M. abscessus* cords, which are thought to affect the outcome of the infection.

RFB treatment enhances protection of zebrafish infected with *M. abscessus*. *In vivo* drug efficacy has previously been well described using the zebrafish model of infection (41, 44, 45). Initial experiments indicated that RFB concentrations of ≤ 100 $\mu\text{g/ml}$ (final concentration in fish water) did not interfere with larval development and was well tolerated in embryos when treatment was applied for 4 days with daily drug renewal (Fig. 5A). Higher concentrations of RFB, however, were associated with rapid larval death. As such, only lower RFB doses (≤ 100 $\mu\text{g/ml}$) were used in subsequent studies. Red fluorescent TdTomato-expressing *M. abscessus* (R variant) was microinjected in the caudal vein of embryos at 30 h postfertilization (hpf). RFB was directly added at 1 dpi to the water containing the infected embryos, with RFB-supplemented water changed on a daily basis for 4 days. Embryo survival was moni-

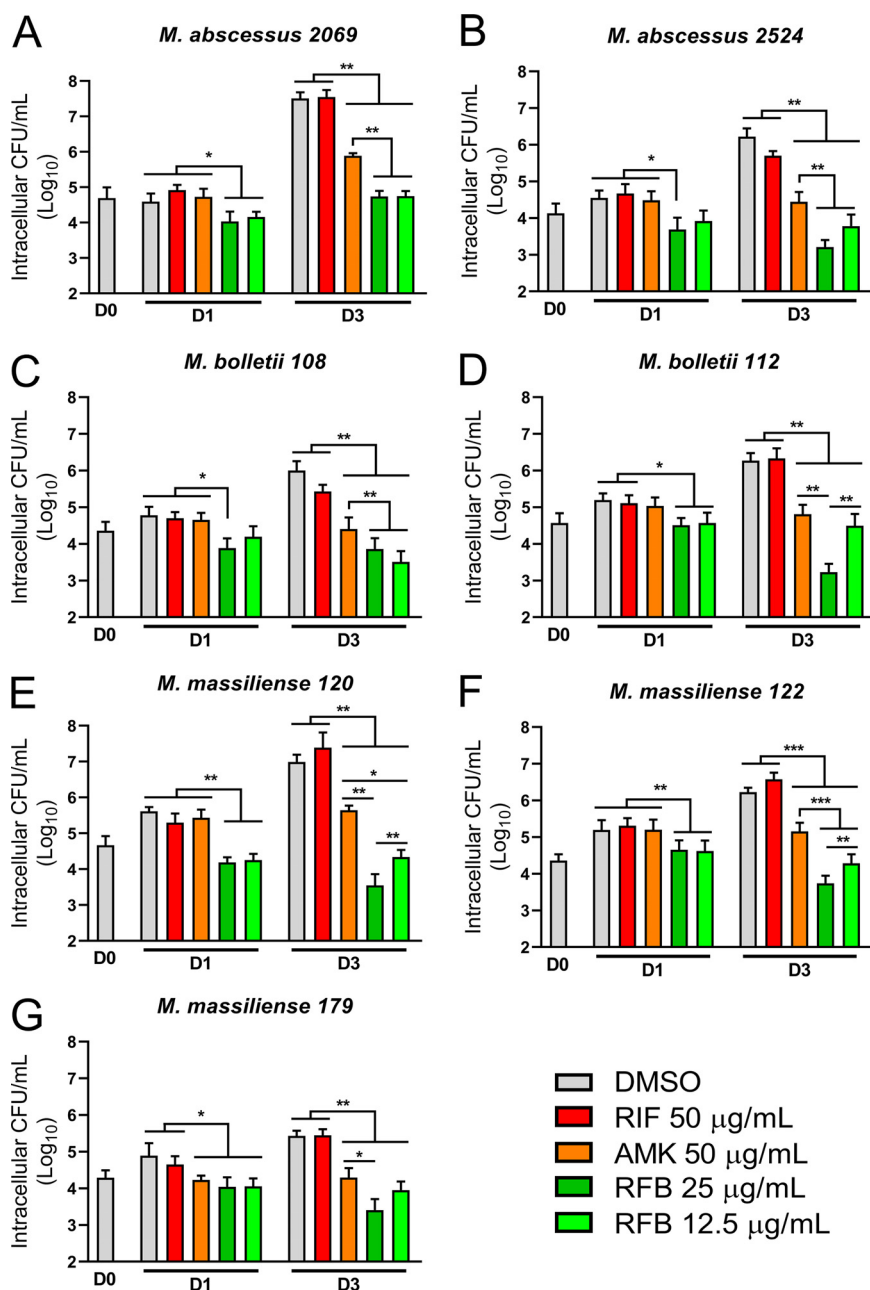


FIG 3 Intracellular activity of RFB on S and R clinical isolates. CFU counts of clinical isolates exposed to 25 and 12.5 µg/ml RFB. Macrophages were infected with *M. abscessus* (A and B), *M. boletii* (C and D), or *M. massiliense* (E to G) clinical strains belonging to S or R morphotypes at an MOI of 2:1 for 3 h prior to treatment with 250 µg/ml AMK for 2 h to kill extracellular bacteria. Following extensive PBS washes, cells were exposed to 50 µg/ml RIF, 50 µg/ml AMK, or 25 or 12.5 µg/ml RFB. CFU were determined at 0, 1, and 3 days postinfection. Data are mean values ± SD for two independent experiments. Data were analyzed using the t test. *, $P \leq 0.05$; **, $P \leq 0.01$; ***, $P \leq 0.001$.

tored and recorded daily for 12 days. No decrease in the survival rate was observed in the presence of 5 µg/ml RFB; however, a significant dose-dependent increase in the survival of embryos exposed to 25 or 50 µg/ml RFB was observed compared to the untreated group (Fig. 5B). When exposed to 50 µg/ml RFB, the highest dose examined in this setting, nearly 80% of the treated embryos survived at 12 dpi, compared to 40% of the untreated group. This clearly indicates that RFB protects zebrafish from *M. abscessus* infection.

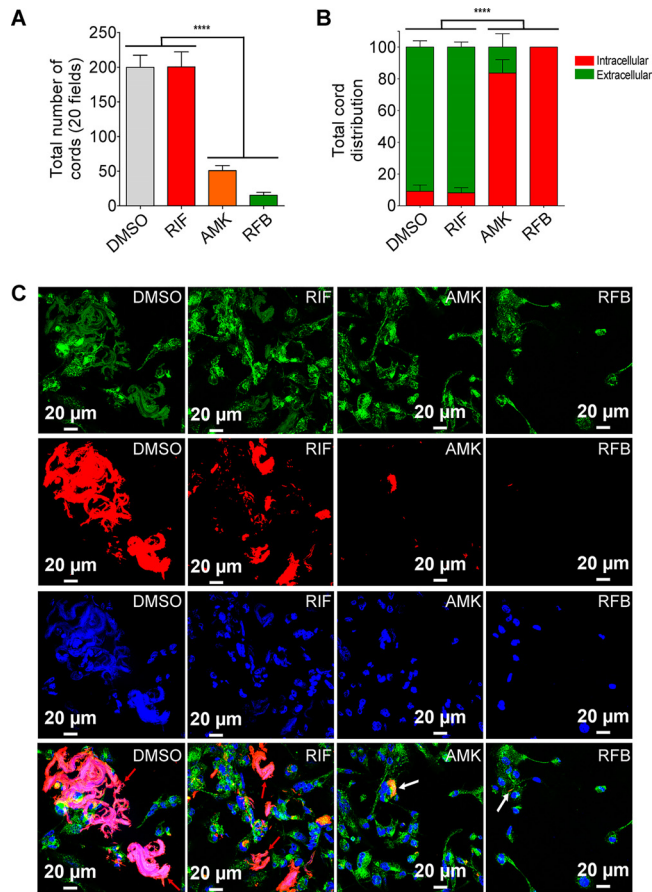


FIG 4 Activity of RFB on extracellular and intracellular cords. (A) Total number of cords displayed in 20 fields at 3 days after infection of macrophages with *M. abscessus* R variant. Data are mean values \pm SD for three independent experiments performed in triplicate. Data were analyzed using one-tailed Mann-Whitney's *t* test. (B) Percentage of cords formed either extracellularly or intracellularly. The two categories were counted at 3 days postinfection in the absence of antibiotics or in the presence of 50 μ g/ml RIF, 50 μ g/ml AMK, or 12.5 μ g/ml RFB. Extracellular or intracellular cords are highlighted using the indicated color codes. Values are means \pm SD for two independent experiments performed each time in triplicate. (C) Four immunofluorescent fields were taken at 3 days postinfection showing the cords formed extracellularly or within macrophages infected with *M. abscessus* R variant expressing Tdtomato (red). Macrophages were infected for 3 days in the presence of DMSO, RIF (50 μ g/ml), AMK (50 μ g/ml), or RFB (12.5 μ g/ml). The macrophage surface was stained using anti-CD63 antibodies (green). The nuclei were stained with DAPI (blue). White arrows indicate intracellular cords, while red arrows indicate extracellular cords. Scale bars represent 20 μ m. Results represent the average of a total of 120 fields per condition. ****, $P \leq 0.0001$.

To test whether RFB exerts an effect on the bacterial burden in zebrafish, we quantified fluorescent pixel counts (FPC) (46). As expected, embryos treated with 50 μ g/ml RFB had significantly decreased bacterial burdens at 2, 4, and 6 dpi compared to the untreated group (Fig. 5C). These results were corroborated by imaging whole embryos, which were characterized by the presence of large abscesses and cords in the brain when left untreated and which were observed much less frequently in the RFB-treated animals despite the presence of single bacilli or small aggregated bacteria (Fig. 5D).

RFB treatment reduces abscess formation by *M. abscessus* in zebrafish. Virulence of *M. abscessus* R variants in zebrafish is correlated with the presence of abscesses, particularly in the central nervous system (14, 46). To address whether the enhanced survival of RFB-treated fish is associated with decreased abscess formation, the percentages of abscesses and cords were determined by monitoring abscesses and cords in whole embryos, as reported previously (14, 46). Extracellular cords can be easily distinguished based on their serpentine-like shape and by their size, often greater

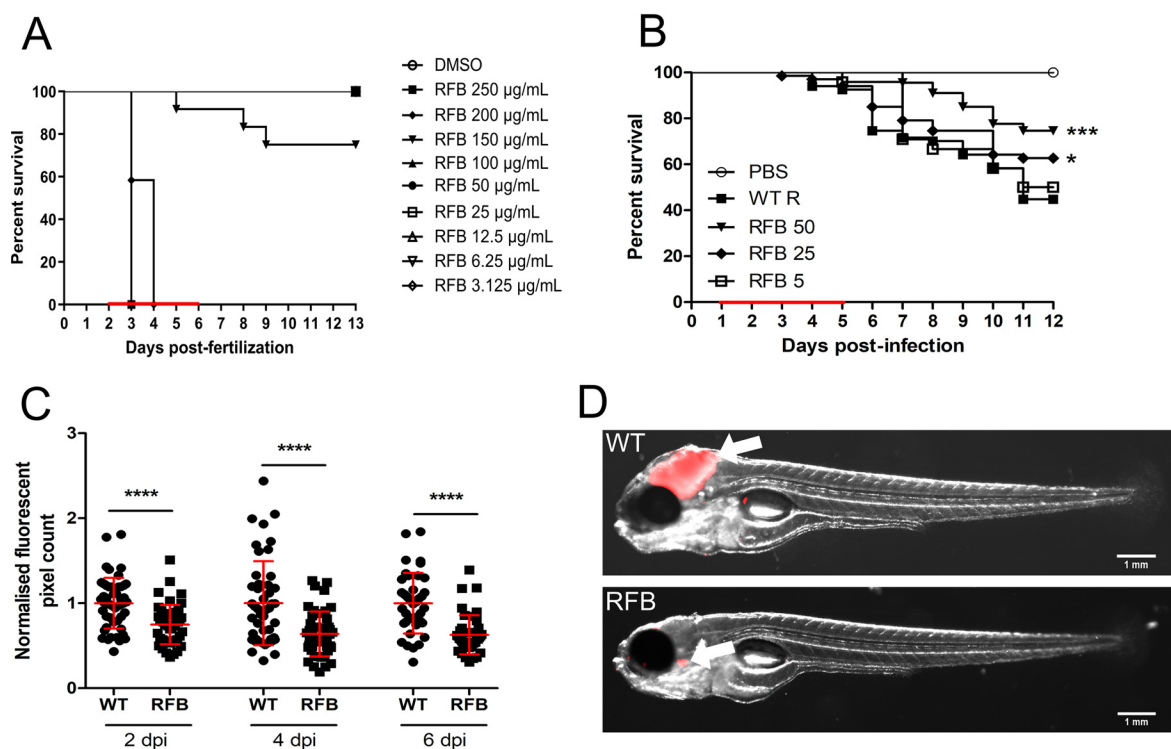


FIG 5 RFB displays high bactericidal activity against *M. abscessus* in an embryonic zebrafish infection model. (A) Groups of uninfected embryos were immersed in water containing increasing concentrations of RFB (ranging from 3.125 to 250 $\mu\text{g}/\text{ml}$) for 4 days. The red bar indicates the duration of treatment. The graph shows the survival of the RFB-treated and untreated (DMSO) embryos over a 12-day period. (B) Zebrafish embryos at 30 h post-fertilization were intravenously infected with approximately 250 to 300 CFU of *M. abscessus* CIP104536^T (R variant) expressing TdTomato ($n = 20$ to 25). A standard PBS injection control was included for each experiment. At 1 dpi, embryos were randomly split into equal groups of approximately 20 embryos per group, and various concentrations of RFB (5 to 50 $\mu\text{g}/\text{ml}$) were added to the water. DMSO was included as a positive control group. RFB was changed daily, after which, embryos were washed twice in fresh embryo water, maintained in embryo water, and monitored daily over a 12-day period. Each treatment group was compared against the untreated infected group with significant differences calculated using the log-rank (Mantel-Cox) statistical test for survival curves. Data shown are the merge of three independent experiments. (C) Bacterial burden was determined at 2, 4, and 6 days postinfection following treatment with either DMSO or 50 $\mu\text{g}/\text{ml}$ RFB. Bacteria were quantified by fluorescent pixel count determination using ImageJ software, with each data point representing a single embryo. Error bars represent standard deviations. Statistical significance was determined using Student's *t* test. The plots represent a pool of 2 independent experiments containing approximately 20 to 25 embryos per group. (D) Representative embryos from the untreated group (WT) (top) and from the treated group with 50 $\mu\text{g}/\text{ml}$ RFB at 6 days postinfection. White arrowheads show TdTomato-expressing bacteria. Scale bars represent 1 mm. *, $P \leq 0.05$; ***, $P \leq 0.001$; ****, $P \leq 0.0001$.

compared to the size of the surrounding macrophages and neutrophils. Exposure of infected embryos to 50 $\mu\text{g}/\text{ml}$ RFB was accompanied by a significant decrease in the proportion of embryos with cords (Fig. 6A) at 4 dpi and the number of embryos with abscesses (Fig. 6B) at 4 and 6 dpi. This decrease in the physiopathological signs of RFB-treated larvae correlates also with the FPC analysis and whole-embryo imaging (Fig. 6C and D). Overall, these results demonstrate that RFB reduces the pathophysiology of *M. abscessus* infection in zebrafish larvae and protects them from bacterial killing.

DISCUSSION

Treatment success of infections caused by *M. abscessus* is unacceptably low even upon prolonged, multidrug chemotherapy with a significant risk of severe toxic side effects. Although RIF is used as a first-line drug against *M. tuberculosis*, it has no activity against *M. abscessus*. While ADP ribosyltransferases can utilize both RIF and RFB as substrates (47), a lower catalytic efficiency with RFB may explain its greater potency against *M. abscessus*. Our study supports and extends previous investigations highlighting the potential of RFB against *M. abscessus* *in vitro* against a wide panel of *M. abscessus* complex clinical isolates (31, 32, 48, 49). We found, however, that our MIC values were higher than those observed in previous investigations (31, 32). In our study,

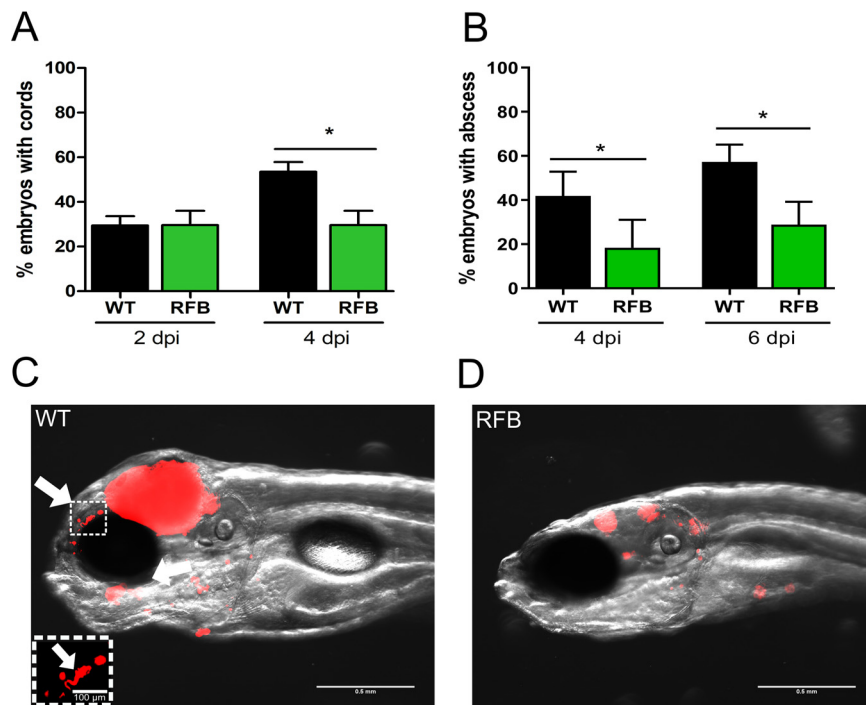


FIG 6 RFB reduces the pathophysiological traits of *M. abscessus* infection in zebrafish embryos. (A) Proportion of embryos with cords at 2 and 4 days postinfection in infected embryos that were either untreated or treated with 50 $\mu\text{g/ml}$ RFB (250 to 300 CFU, $n = 30$). Data were analyzed using an unpaired Student's *t* test. Data shown are the mean of three independent experiments \pm SD. (B) Total percentage of embryos with abscesses at 4 and 6 dpi in infected embryos that were either untreated or treated with 50 $\mu\text{g/ml}$ RFB (250 to 300 CFU, $n = 30$). Data were analyzed using an unpaired Student's *t* test. Data shown are the mean of three independent experiments \pm SD. (C and D) Representative zebrafish images of untreated (WT) embryos and those treated with 50 $\mu\text{g/ml}$ RFB at 6 dpi. Scale bar represents 0.5 mm. White arrows indicate extracellular cords. The white box highlights a large extracellular cord based on the size and morphology, with the scale bar representing 100 μm . Red overlay represents *M. abscessus* expressing TdTomato. *, $P \leq 0.05$.

following the Clinical and Laboratory Standard Institute (CLSI) guidelines, MIC were determined in CaMHB, while Aziz et al. showed that MIC values were 2- to 3-fold higher in CaMHB compared to Middlebrook 7H9 (31), clearly implicating an effect of medium on RFB susceptibility testing. In line with these results, we noticed important variations in the MIC values depending on the culture medium used for RFB susceptibility assessments. It is also noteworthy that the growth curve of the untreated S strain is different from that of the R strain, which is very likely linked to the highly aggregative surface properties typifying the R strain, which in contrast to the S strain, produces very clumpy and corded cultures in broth medium (10, 46, 50). As a consequence, colonies on agar plates very likely emerge from aggregated bacteria rather than individual bacilli, explaining why the CFU counts were significantly lower in both cultures. Thus, the CFU counts of the R strain do not accurately reflect the absolute number of living bacilli in the culture. We also selected RFB-resistant mutants and identified mutations in *rpoB*, which is known as the primary target of rifampin in *M. tuberculosis* (51). Interestingly, the mutations identified are part of the rifampin-resistance-determining region (RRDR), an 81-bp central segment corresponding to codons 426 to 452 in *M. tuberculosis* that harbors the vast majority of *rpoB* mutations associated with resistance to RIF (51). It is noteworthy that S452L corresponds to one of the most frequently mutated coding regions in the *rpoB* gene in *M. tuberculosis* (S450L replacement) (51). Together, these results suggest that RpoB is very likely the target of RFB in *M. abscessus*.

Among the various studies reporting the activity of RFB against *M. abscessus in vitro*, very few discriminated the activity of RFB against the S or R morphotypes. Here, we found that the type strain CIP104536^T S was reproducibly more resistant to RFB than its

R counterpart. Supporting these results, deletion of *mmpL4b* in the S genetic background, resulting in an R morphotype lacking GPL (13, 37), increased susceptibility to RFB. Conversely, functional complementation of the *mmpL4b* mutant, restoring the S morphotype and GPL production (13, 37), partially rescued the higher MIC. This highlights the influence of the outermost GPL layer on susceptibility to RFB. Previously, the activity of other inhibitors was shown to be dependent on the presence or absence of GPL in *M. abscessus* (17, 18). A logical explanation is that the GPL layer protects the bacilli from the penetration of drugs. The absence of GPL may enhance the permeability of the cell wall and accumulation of the drug inside the bacteria. However, one cannot exclude the possibility that MmpL4b, like other MmpL transporters, can act as an efflux pump (52–54) and may participate in the extrusion of RFB in *M. abscessus* S, resulting in higher MIC. The implication of efflux pumps in resistance to RFB has been investigated, whereby the overexpression of MAB_1409c (a homologue of the *M. tuberculosis* Rv1258c) resulted in increased resistance to RFB in the R variant of *M. abscessus*. This effect was not observed in the S strain overexpressing MAB_1409c, presumably because of the already elevated MIC of the parental S strain toward RFB. However, while the increased susceptibility of the R strain compared to the S strain was true with respect to the type strain, this was not observed for all clinical strains tested. The heterogeneity of the clinical strains in response to RFB treatment cannot be simply explained by the presence or absence of GPL but may also include additional determinants of resistance to RFB (48), such as differences in the expression level of Arr_{Mab} or the expression of Rox monooxygenases, known to inactivate RIF in other bacterial species as proposed earlier (55). This, however, requires further investigation in follow-up studies.

One unanticipated finding from this study relies on the fact that, although S and R variants respond differently to RFB treatment *in vitro*, this was not the case against the intracellularly residing *M. abscessus*. We found that, using a macrophage model of infection, the isogenic S and R type strains responded equally well to treatment with 12.5 µg/ml RFB, largely exceeding the results obtained with AMK, a drug displaying weak intracellular activity (56). These observations are reminiscent of other studies indicating that various naphthalenic ansamycins, including RIF, differ profoundly in their capacity to kill extracellular *Staphylococcus aureus*, although there were few differences observed between them in promoting human macrophages to kill phagocytosed bacteria (57). There is no simple explanation for why *M. abscessus* S is as efficiently killed as *M. abscessus* R inside the cells. A plausible explanation may be that the stress response inside macrophages alters the composition/architecture of the cell wall of *M. abscessus*, thereby affecting the GPL layer and/or permeability of the S variant. It has been shown that the GPL layer significantly influences the hydrophobic surface properties (58), potentially impacting the adhesion and the uptake of the bacilli. Furthermore, electron microscopy observations revealed that the electron translucent zone (ETZ) that fills the entire space between the phagosome and the bacterial surface relies on GPL production in the S variant (11). Alternatively, RFB may directly induce the antimycobacterial activity of the macrophage, which in turn, translates into a rapid killing of the phagocytosed bacteria, regardless of their morphotype. Overall, these results suggest that the MIC values of RFB are not indicative of the intraphagocytic killing of *M. abscessus* and highlight the importance of testing the efficacy of drugs in a macrophage infection model.

Cords and abscesses are pathophysiological markers of *M. abscessus* infection, as revealed using the zebrafish model of infection (44). In particular, extracellular cords, due to their size, prevent the bacilli from being phagocytosed by macrophages and neutrophils, representing an important mechanism of immune evasion (14, 46). We demonstrate here that treatment of infected macrophages was associated with reduced intra- and extracellular cording of the R variant. It is very likely that RFB prevents cording, as a consequence of the inhibition of bacterial replication/killing. Cords are a hallmark of virulence of the R variant of *M. abscessus*, as emphasized by a deletion mutant of MAB_4780, encoding a dehydratase, displaying a pronounced defect in

cording and a highly attenuated phenotype in macrophages (59). Importantly, we observed also a significant decrease in the number of embryos with cords following RFB treatment in infected zebrafish. It is worth highlighting that in the presence of RFB, there is no change in the number of embryos with cords between 2 and 4 dpi, suggesting that while RFB does not degrade or modify the bacterial cord structure, it likely prevents the formation of additional cords. Moreover, the effect of RFB on cord reduction is particularly interesting, as it may prevent the subsequent formation of abscesses (14), considered a marker of the severity of the disease. Consistent with this hypothesis, a marked decrease in abscess formation was observed in RFB-treated zebrafish embryos. Overall, this work supports the practicality of zebrafish as a preclinical model to evaluate in real time the bactericidal efficacy of RFB against *M. abscessus* infection in the sole context of innate immunity.

In summary, although there is a clear lack of bactericidal activity of drugs against *M. abscessus* (60), these findings support the high level of activity of RFB against *M. abscessus* *in vivo* and *in vitro*. Our results further emphasize the efficacy of RFB against both extracellular and intracellular forms of *M. abscessus*, both coexisting in infected patients, as well as a protective effect in an animal model of *M. abscessus* infection. In addition, we provided further evidence that S and R variants are differentially susceptible to RFB, likely due to the GPL layer; however, the MIC values are not predictive of intracellular drug efficacy.

Together with the fact that RFB is an FDA-approved drug that is already used to treat tuberculosis (61) and *M. avium* infections (62) with favorable pharmacological properties (63), our data strengthen the view that RFB should be considered a repurposing drug candidate for the treatment of *M. abscessus* infections. Importantly, recent work has shown that RFB is synergistic in combination with other antimicrobials, such as clarithromycin, imipenem, and tigecycline, and significantly improves the activity of imipenem-tedizolid drug combinations (32, 42, 49, 64). Future studies are required to test whether these RFB combinations are effective against *M. abscessus* pulmonary infections.

MATERIALS AND METHODS

Mycobacterial strains and growth conditions. *M. abscessus* CIP104536^T, *M. boletii* CIP108541^T, and *M. massiliense* CIP108297^T reference strains and clinical isolates from CF and non-CF patients were reported previously (65, 66). Strains were routinely grown and maintained at 30°C in Middlebrook 7H9 broth (BD Difco) supplemented with 0.05% Tween 80 (Sigma-Aldrich) and 10% oleic acid, albumin, dextrose, and catalase (OADC enrichment; BD Difco) (7H9^{T/OADC}) or on Middlebrook 7H10 agar (BD Difco) containing 10% OADC enrichment (7H10^{OADC}) and in the presence of antibiotics when required. For drug susceptibility testing, bacteria were grown in cation-adjusted Mueller-Hinton broth (CaMHB; Sigma-Aldrich). RFB was purchased from two independent commercial sources (AduoQ Bioscience and Sellckchem) and dissolved in DMSO.

Drug susceptibility testing. The MICs were determined according to the CLSI guidelines (67). The broth microdilution method was used in CaMHB with an inoculum of 5×10^6 CFU/ml in the exponential growth phase. The bacterial suspension was seeded in 100- μ l volumes in all of the wells of a 96-well plate, except for the first column, to which 198 μ l of the bacterial suspension was added. In the first column, 2 μ l of drug at its highest concentration was added to the first well containing 198 μ l of bacterial suspension. Then, 2-fold serial dilutions were carried out, and the plates were incubated for 3 to 5 days at 30°C. MICs were recorded by visual inspection. Assays were completed in triplicate in three independent experiments.

Growth inhibition kinetics. To monitor the growth inhibition of *M. abscessus* CIP104536^T S and R, 96-well plates were set up as for MIC determination, and serial dilutions of the bacterial suspensions exposed to increasing concentrations of RFB were plated on LB agar plates after 0, 24, 48, and 72 h. CFU were counted after 4 days of incubation at 30°C. Results from each drug concentration are representative of at least 2 independent experiments.

Cytotoxicity assay. THP-1 cells were differentiated with phorbol myristate acetate (PMA) for 48 h and exposed to decreasing concentrations of either RFB or RIF (starting at 200 μ g/ml) for an additional 72 h at 37°C with 5% CO₂. Following incubation, 10% (vol/vol) resazurin dye was added to each well and left to incubate for 4 h at 37°C and 5% CO₂. Data were acquired using a fluorescent plate reader (excitation, 540 nm; emission, 590 nm). DMSO was included as a negative control, while SDS was included as a positive control.

Intracellular killing assay. Human THP-1 monocytes were grown in RPMI medium supplemented with 10% fetal bovine serum (Sigma-Aldrich) (RPMI^{FBS}) and incubated at 37°C in the presence of 5% CO₂. Cells were differentiated into macrophages in the presence of 20 ng/ml PMA in 24-well flat-bottom tissue culture microplates (1×10^5 cells/well) and incubated for 48 h at 37°C with 5% CO₂. Infection with clinical

isolates or *M. abscessus* harboring pTEC27 fluorescent TdTomato was carried out at 37°C in the presence of 5% CO₂ for 3 h at a multiplicity of resistance (MOI) of 2:1. After extensive washing with 1× phosphate-buffered saline (PBS), cells were incubated with RPMI^{FBS} containing 250 µg/ml amikacin for 2 h and washed again with PBS prior to the addition of 500 µl RPMI^{FBS} containing DMSO (negative control), 500 µl RPMI^{FBS} containing 50 µg/ml of RIF or AMK, or 12.5 µg/ml of RFB. Macrophages were washed with PBS and lysed with 100 µl of 1% Triton X-100 at required time points. Serial dilutions of macrophage lysates were plated onto LB agar plates, and colonies were counted to determine intracellular CFU.

Microscopy-based infectivity assays. Monocytes were differentiated into macrophages (THP-1) in the presence of PMA and were grown on coverslips in 24-well plates at a density of 10⁵ cells/ml for 48 h at 37°C with 5% CO₂ prior to infection with Tdtomato expressing *M. abscessus* for 3 h at an MOI of 2:1. After washing and AMK treatment to remove the extracellular bacilli, macrophages were exposed to DMSO (negative control), 50 µg/ml RIF or AMK, or 12.5 µg/ml RFB and fixed at 0, 1, and 3 days postinfection with 4% paraformaldehyde in PBS for 20 min. Cells were then permeabilized using 0.2% Triton X-100 for 20 min, blocked with 2% BSA in PBS supplemented with 0.2% Triton X-100 for 20 min, incubated with anti-CD63 antibodies (Becton, Dickinson; dilution, 1:1,000) for 1 h and with an Alexa Fluor 488-conjugated anti-mouse secondary antibody (Molecular Probes, Invitrogen). After 5 min of incubation with DAPI (dilution, 1:1,000), cells were mounted onto microscope slides using Immu-mount (Calbiochem) and examined with an epifluorescence microscope using a 63× lens objective. The average proportion of macrophages containing <5, 5 to 10, or >10 bacilli were quantified using Zeiss AxioVision software. Images were acquired by focusing on combined signals (CD63 in green and red fluorescent *M. abscessus*) and captured on a Zeiss Axio Imager confocal microscope equipped with a 63× oil objective and processed using Zeiss AxioVision software. Quantification and scoring of the numbers of bacilli present within macrophages were performed using ImageJ. Equal parameters for the capture and scoring of images were consistently applied to all samples. For each condition, approximately 1,000 infected macrophages were analyzed. The presence of the intra- or extracellular cords within or among the macrophages infected with the R morphotype strain were treated in the presence of DMSO, RIF, RFB, or AMK at the concentrations previously described, counted, and imaged using confocal microscopy.

Assessment of RFB efficacy in infected zebrafish. Experiments in zebrafish were conducted according to the Comité d’Ethique pour l’Expérimentation Animale de la Région Languedoc Roussillon under the reference number CEEALR36-1145. Experiments were performed using the *golden* mutant (68). Embryos were obtained and maintained as described (14). Embryo age is expressed as hours postfertilization (hpf). Red fluorescent *M. abscessus* CIP104536^T (R) expressing TdTomato was prepared and microinjected in the caudal vein (2 to 3 nl containing ≈100 bacteria/nl) in 30 hpf embryos previously dechorionated and anesthetized with tricaine, as described earlier (46). The bacterial inoculum was checked *a posteriori* by injection of 2 nl in sterile phosphate-buffered saline with Tween (PBST) and plating on 7H10^{OADC}. Infected embryos were transferred into 24-well plates (2 embryos/well) and incubated at 28.5°C to monitor kinetics of infection and embryo survival. Survival curves were determined by counting dead larvae daily for up to 12 days, with the experiment concluded when uninfected embryos started to die. RFB treatment of infected embryos and uninfected embryos commenced at 24 hours postinfection (hpi) for 4 days. The drug-containing solution was renewed daily. Bacterial loads in live embryos were determined by anesthetizing embryos in tricaine as previously described (44), mounting on 3% (wt/vol) methylcellulose solution, and taking fluorescent images using a Zeiss Axio Zoom.V16 coupled with an Axiocam 503 mono (Zeiss). Fluorescence pixel count (FPC) measurements were determined using the “analyze particles” function in ImageJ (46). Bacterial cords were identified based on the size and shape of fluorescent bacteria within the live zebrafish embryo, vastly exceeding the surrounding size and shape of neighboring cells. All experiments were completed at least three times independently.

Overexpression of MAB_1409c in *M. abscessus*. Overexpression was achieved by PCR amplification of *MAB_1409c* (*tap*) in fusion with an HA tag using genomic DNA and the forward primer (5'-gagaCAA TTGCCATGTCCACTCCGACGGCGGATTC-3'; MfeI) and reverse primer (5'-gagaGTTAACCTAAGCGTAATCTG GAACATCGTATGGGTACCGAGTTGGTTCCTTGTCGGGCT-3'; HpaI). The amplified product was digested with MfeI/HpaI and ligated into the MfeI/HpaI-restricted pMV306 integrative vector to generate pMV306-*MAB_1409c*-HA, where *MAB_1409c*-HA is under the control of the *hsp60* promoter. The construct was sequenced and electroporated into *M. abscessus* S and R.

Selection of resistant *M. abscessus* mutants and target identification. Exponentially growing *M. abscessus* CIP104536^T R cultures were plated on LB agar containing either 25 or 50 µg/ml RFB. After 1 week of incubation at 37°C, two individual colonies from each RFB concentration were selected, grown in CaMHB, individually assessed for MIC determination, and scored for resistance to RFB. Identification of SNPs in the resistant strains was completed by PCR amplification using *rpoB_f* 5'-TCAGTGGGGCTGGTT AG-3' and *rpoB_r* 5'-AAAACATCGCAGATGCGC-3' to produce a 3,541-bp amplicon for full coverage sequencing of the *rpoB* gene.

Western blotting. Bacteria were harvested, resuspended in PBS, and disrupted by bead-beating with 1-mm-diameter glass beads. The protein concentration in the lysates was determined, and equal amounts of proteins (100 µg) were subjected to SDS-PAGE. Proteins were transferred to a nitrocellulose membrane. For detection of Tap-HA and KasA (loading control), the membranes were incubated for 1 h with either the rat anti-HA or rat anti-KasA antibodies (dilution, 1:2,000), washed, and subsequently incubated with goat anti-rat antibodies conjugated to HRP (Abcam; dilution, 1:5,000). The signal was revealed using the ChemiDoc MP system (Bio-Rad).

Statistical analyses. Statistical analyses were performed on Prism 5.0 (GraphPad) and detailed for each figure legend. *, $P \leq 0.05$, **, $P \leq 0.01$, ***, $P \leq 0.001$, ****, $P \leq 0.0001$.

SUPPLEMENTAL MATERIAL

Supplemental material is available online only.

SUPPLEMENTAL FILE 1, PDF file, 0.8 MB.

ACKNOWLEDGMENTS

M.D.J. received a postdoctoral fellowship granted by Labex EpiGenMed, an “Investissements d’Avenir” program (ANR-10-LABX-12-01). This study was supported by the Association Gregory Lemarchal and Vaincre la Mucoviscidose (RIF20180502320) to L.K.

We have no conflict of interest to declare.

REFERENCES

- Johansen MD, Herrmann J-L, Kremer L. 2020. Non-tuberculous mycobacteria and the rise of *Mycobacterium abscessus*. *Nat Rev Microbiol* 18:392–407. <https://doi.org/10.1038/s41579-020-0331-1>.
- Cowman S, van Ingen J, Griffith DE, Loebinger MR. 2019. Non-tuberculous mycobacterial pulmonary disease. *Eur Respir J* 54:1900250. <https://doi.org/10.1183/13993003.00250-2019>.
- Jönsson BE, Gilljam M, Lindblad A, Ridell M, Wold AE, Welinder-Olsson C. 2007. Molecular epidemiology of *Mycobacterium abscessus*, with focus on cystic fibrosis. *J Clin Microbiol* 45:1497–1504. <https://doi.org/10.1128/JCM.02592-06>.
- Esther CR, Esserman DA, Gilligan P, Kerr A, Noone PG. 2010. Chronic *Mycobacterium abscessus* infection and lung function decline in cystic fibrosis. *J Cyst Fibros* 9:117–123. <https://doi.org/10.1016/j.jcf.2009.12.001>.
- Catherinot E, Roux A-L, Macheras E, Hubert D, Matmar M, Dannhoffer L, Chinet T, Morand P, Poyart C, Heym B, Rottman M, Gaillard J-L, Herrmann J-L. 2009. Acute respiratory failure involving an R variant of *Mycobacterium abscessus*. *J Clin Microbiol* 47:271–274. <https://doi.org/10.1128/JCM.01478-08>.
- Adekambi T, Sassi M, van Ingen J, Drancourt M. 2017. Reinstating *Mycobacterium massiliense* and *Mycobacterium bolletii* as species of the *Mycobacterium abscessus* complex. *Int J Syst Evol Microbiol* 67:2726–2730. <https://doi.org/10.1099/ijsem.0.002011>.
- Koh W-J, Jeon K, Lee NY, Kim B-J, Kook Y-H, Lee S-H, Park YK, Kim CK, Shin SJ, Huit G, Daley CL, Kwon OJ. 2011. Clinical significance of differentiation of *Mycobacterium massiliense* from *Mycobacterium abscessus*. *Am J Respir Crit Care Med* 183:405–410. <https://doi.org/10.1164/rccm.201003-0395OC>.
- Howard ST, Rhoades E, Recht J, Pang X, Alsup A, Kolter R, Lyons CR, Byrd TF. 2006. Spontaneous reversion of *Mycobacterium abscessus* from a smooth to a rough morphotype is associated with reduced expression of glycopeptidolipid and reacquisition of an invasive phenotype. *Microbiology* 152:1581–1590. <https://doi.org/10.1099/mic.0.28625-0>.
- Gutiérrez AV, Viljoen A, Ghigo E, Herrmann J-L, Kremer L. 2018. Glycopeptidolipids, a double-edged sword of the *Mycobacterium abscessus* complex. *Front Microbiol* 9:1145. <https://doi.org/10.3389/fmicb.2018.01145>.
- Roux A-L, Viljoen A, Bah A, Simeone R, Bernut A, Laencina L, Deramaudt T, Rottman M, Gaillard J-L, Majlessi L, Brosch R, Girard-Misguich F, Vergne I, de Chastellier C, Kremer L, Herrmann J-L. 2016. The distinct fate of smooth and rough *Mycobacterium abscessus* variants inside macrophages. *Open Biol* 6:160185. <https://doi.org/10.1098/rsob.160185>.
- Bernut A, Viljoen A, Dupont C, Sapriel G, Blaise M, Bouchier C, Brosch R, de Chastellier C, Herrmann J-L, Kremer L. 2016. Insights into the smooth-to-rough transition in *Mycobacterium bolletii* unravels a functional Tyr residue conserved in all mycobacterial MmpL family members. *Mol Microbiol* 99:866–883. <https://doi.org/10.1111/mmi.13283>.
- Sánchez-Chardi A, Olivares F, Byrd TF, Julián E, Brambila C, Luquin M. 2011. Demonstration of cord formation by rough *Mycobacterium abscessus* variants: implications for the clinical microbiology laboratory. *J Clin Microbiol* 49:2293–2295. <https://doi.org/10.1128/JCM.02322-10>.
- Nessar R, Reytrat J-M, Davidson LB, Byrd TF. 2011. Deletion of the *mmpL4b* gene in the *Mycobacterium abscessus* glycopeptidolipid biosynthetic pathway results in loss of surface colonization capability, but enhanced ability to replicate in human macrophages and stimulate their innate immune response. *Microbiology* 157:1187–1195. <https://doi.org/10.1099/mic.0.046557-0>.
- Bernut A, Herrmann J-L, Kissa K, Dubremetz J-F, Gaillard J-L, Lutfalla G, Kremer L. 2014. *Mycobacterium abscessus* cording prevents phagocytosis and promotes abscess formation. *Proc Natl Acad Sci U S A* 111:E943–952. <https://doi.org/10.1073/pnas.1321390111>.
- Park IK, Hsu AP, Tettelin H, Shallom SJ, Drake SK, Ding L, Wu U-I, Adamo N, Prevots DR, Olivier KN, Holland SM, Sampaio EP, Zelazny AM. 2015. Clonal diversification and changes in lipid traits and colony morphology in *Mycobacterium abscessus* clinical isolates. *J Clin Microbiol* 53:3438–3447. <https://doi.org/10.1128/JCM.02015-15>.
- Pawlik A, Garnier G, Orgeur M, Tong P, Lohan A, Le Chevalier F, Sapriel G, Roux A-L, Conlon K, Honoré N, Dillies M-A, Ma L, Bouchier C, Coppée J-Y, Gaillard J-L, Gordon SV, Loftus B, Brosch R, Herrmann JL. 2013. Identification and characterization of the genetic changes responsible for the characteristic smooth-to-rough morphotype alterations of clinically persistent *Mycobacterium abscessus*. *Mol Microbiol* 90:612–629. <https://doi.org/10.1111/mmi.12387>.
- Madani A, Ridenour JN, Martin BP, Paudel RR, Abdul Basir A, Le Moigne V, Herrmann J-L, Audebert S, Camoin L, Kremer L, Spilling CD, Cnaan S, Cavalier J-F. 2019. Cyclosporins and Cyclophosphamide analogues as multitarget inhibitors that impair growth of *Mycobacterium abscessus*. *ACS Infect Dis* 5:1597–1608. <https://doi.org/10.1021/acsinfecdis.9b00172>.
- Lavollay M, Dubée V, Heym B, Herrmann J-L, Gaillard J-L, Gutmann L, Arthur M, Mainardi J-L. 2014. *In vitro* activity of cefoxitin and imipenem against *Mycobacterium abscessus* complex. *Clin Microbiol Infect* 20:O297–O300. <https://doi.org/10.1111/1469-0691.12405>.
- Nessar R, Cambau E, Reytrat JM, Murray A, Gicquel B. 2012. *Mycobacterium abscessus*: a new antibiotic nightmare. *J Antimicrob Chemother* 67:810–818. <https://doi.org/10.1093/jac/dkr578>.
- van Ingen J, Boeree MJ, van Soolingen D, Mouton JW. 2012. Resistance mechanisms and drug susceptibility testing of nontuberculous mycobacteria. *Drug Resist Updat* 15:149–161. <https://doi.org/10.1016/j.drug.2012.04.001>.
- Brown-Elliott BA, Nash KA, Wallace RJ. 2012. Antimicrobial susceptibility testing, drug resistance mechanisms, and therapy of infections with nontuberculous mycobacteria. *Clin Microbiol Rev* 25:545–582. <https://doi.org/10.1128/CMR.05030-11>.
- Lopeman R, Harrison J, Desai M, Cox J. 2019. *Mycobacterium abscessus*: environmental bacterium turned clinical nightmare. *Microorganisms* 7:90. <https://doi.org/10.3390/microorganisms7030090>.
- Luthra S, Rominski A, Sander P. 2018. The role of antibiotic-target-modifying and antibiotic-modifying enzymes in *Mycobacterium abscessus* drug resistance. *Front Microbiol* 9:2179. <https://doi.org/10.3389/fmicb.2018.02179>.
- Wu M-L, Aziz DB, Dartois V, Dick T. 2018. NTM drug discovery: status, gaps and the way forward. *Drug Discov Today* 23:1502–1519. <https://doi.org/10.1016/j.drudis.2018.04.001>.
- Griffith DE, Aksamit T, Brown-Elliott BA, Catanzaro A, Daley C, Gordin F, Holland SM, Horsburgh R, Huit G, Iademarco MF, Iseman M, Olivier K, Ruoss S, von Reyn CF, Wallace RJ, Winthrop K, ATS Mycobacterial Diseases Subcommittee, American Thoracic Society, Infectious Disease Society of America. 2007. An official ATS/IDSA statement: diagnosis, treatment, and prevention of nontuberculous mycobacterial diseases. *Am J*

- Respir Crit Care Med 175:367–416. <https://doi.org/10.1164/rccm.200604-571ST>.
26. Floto RA, Olivier KN, Saiman L, Daley CL, Herrmann J-L, Nick JA, Noone PG, Bilton D, Corris P, Gibson RL, Hempstead SE, Koetz K, Sabadosa KA, Sermet-Gaudelus I, Smyth AR, van Ingen J, Wallace RJ, Winthrop KL, Marshall BC, Haworth CS. 2016. US Cystic Fibrosis Foundation and European Cystic Fibrosis Society consensus recommendations for the management of non-tuberculous mycobacteria in individuals with cystic fibrosis: executive summary. *Thorax* 71:88–90. <https://doi.org/10.1136/thoraxjnl-2015-207983>.
 27. Daley CL, Iaccarino JM, Lange C, Cambau E, Wallace RJ, Andrejak C, Böttger EC, Brozek J, Griffith DE, Guglielmetti L, Huitt GA, Knight SL, Leitman P, Marras TK, Olivier KN, Santin M, Stout JE, Tortoli E, van Ingen J, Wagner D, Winthrop KL. 2020. Treatment of nontuberculous mycobacterial pulmonary disease: an official ATS/ERS/ESCMID/IDSA clinical practice guideline. *Eur Respir J* 56:2000535. <https://doi.org/10.1183/13993003.00535-2020>.
 28. Wallace RJ, Dukart G, Brown-Elliott BA, Griffith DE, Scerpella EG, Marshall B. 2014. Clinical experience in 52 patients with tigecycline-containing regimens for salvage treatment of *Mycobacterium abscessus* and *Mycobacterium chelonae* infections. *J Antimicrob Chemother* 69:1945–1953. <https://doi.org/10.1093/jac/dku062>.
 29. Roux A-L, Catherinot E, Soismier N, Heym B, Bellis G, Lemonnier L, Chiron R, Fauroux B, Le Bourgeois M, Munck A, Pin I, Sermet I, Gutierrez C, Véziris N, Jarlier V, Cambau E, Herrmann J-L, Guillemot D, Gaillard J-L, OMA Group. 2015. Comparing *Mycobacterium massiliense* and *Mycobacterium abscessus* lung infections in cystic fibrosis patients. *J Cyst Fibros* 14:63–69. <https://doi.org/10.1016/j.jcf.2014.07.004>.
 30. Daniel-Wayman S, Abate G, Barber DL, Bermudez LE, Coler RN, Cynamon MH, Daley CL, Davidson RM, Dick T, Floto RA, Henkle E, Holland SM, Jackson M, Lee RE, Nuernberger EL, Olivier KN, Ordway DJ, Prevots DR, Sacchetti JC, Salfinger M, Sasseti CM, Sizemore CF, Winthrop KL, Zelazny AM. 2019. Advancing translational science for pulmonary non-tuberculous mycobacterial infections. A road map for research. *Am J Respir Crit Care Med* 199:947–951. <https://doi.org/10.1164/rccm.201807-1273PP>.
 31. Aziz DB, Low JL, Wu M-L, Gengenbacher M, Teo JWP, Dartois V, Dick T. 2017. Rifabutin is active against *Mycobacterium abscessus* complex. *Antimicrob Agents Chemother* 61:e00155-17. <https://doi.org/10.1128/AAC.00155-17>.
 32. Pryjma M, Burian J, Thompson CJ. 2018. Rifabutin acts in synergy and is bactericidal with frontline *Mycobacterium abscessus* antibiotics clarithromycin and tigecycline, suggesting a potent treatment combination. *Antimicrob Agents Chemother* 62:e00283-18. <https://doi.org/10.1128/AAC.00283-18>.
 33. Rominski A, Roditschkeff A, Selchow P, Böttger EC, Sander P. 2017. Intrinsic rifamycin resistance of *Mycobacterium abscessus* is mediated by ADP-ribosyltransferase MAB_0591. *J Antimicrob Chemother* 72:376–384. <https://doi.org/10.1093/jac/dkw466>.
 34. Dick T, Shin SJ, Koh W-J, Dartois V, Gengenbacher M. 2019. Rifabutin is active against *Mycobacterium abscessus* in mice. *Antimicrob Agents Chemother* 64:e01943-19. <https://doi.org/10.1128/AAC.01943-19>.
 35. Lefebvre A-L, Dubée V, Cortes M, Dorcène D, Arthur M, Mainardi J-L. 2016. Bactericidal and intracellular activity of β -lactams against *Mycobacterium abscessus*. *J Antimicrob Chemother* 71:1556–1563. <https://doi.org/10.1093/jac/dkw022>.
 36. Story-Roller E, Maggioncalda EC, Lamichhane G. 2019. Select β -lactam combinations exhibit synergy against *Mycobacterium abscessus* *in vitro*. *Antimicrob Agents Chemother* 63:e00614-19. <https://doi.org/10.1128/AAC.02613-18>.
 37. Medjahed H, Reyat J-M. 2009. Construction of *Mycobacterium abscessus* defined glycopeptidolipid mutants: comparison of genetic tools. *Appl Environ Microbiol* 75:1331–1338. <https://doi.org/10.1128/AEM.01914-08>.
 38. Roux A-L, Ray A, Pawlik A, Medjahed H, Etienne G, Rottman M, Catherinot E, Coppée J-Y, Chaoui K, Monsarrat B, Toubert A, Daffé M, Puzo G, Gaillard J-L, Brosch R, Dulphy N, Nigou J, Herrmann J-L. 2011. Overexpression of proinflammatory TLR-2-signalling lipoproteins in hypervirulent mycobacterial variants. *Cell Microbiol* 13:692–704. <https://doi.org/10.1111/j.1462-5822.2010.01565.x>.
 39. Ripoll F, Pasek S, Schenowitz C, Dossat C, Barbe V, Rottman M, Macheras E, Heym B, Herrmann J-L, Daffé M, Brosch R, Risler J-L, Gaillard J-L. 2009. Non mycobacterial virulence genes in the genome of the emerging pathogen *Mycobacterium abscessus*. *PLoS One* 4:e5660. <https://doi.org/10.1371/journal.pone.0005660>.
 40. Balganes M, Dinesh N, Sharma S, Kuruppath S, Nair AV, Sharma U. 2012. Efflux pumps of *Mycobacterium tuberculosis* play a significant role in antituberculosis activity of potential drug candidates. *Antimicrob Agents Chemother* 56:2643–2651. <https://doi.org/10.1128/AAC.06003-11>.
 41. Dupont C, Viljoen A, Thomas S, Roquet-Banères F, Herrmann J-L, Pethe K, Kremer L. 2017. Bedaquiline inhibits the ATP synthase in *Mycobacterium abscessus* and is effective in infected zebrafish. *Antimicrob Agents Chemother* 61:e01225-17. <https://doi.org/10.1128/AAC.01225-17>.
 42. Cheng A, Tsai Y-T, Chang S-Y, Sun H-Y, Wu U-I, Sheng W-H, Chen Y-C, Chang S-C. 2019. *In vitro* synergism of rifabutin with clarithromycin, imipenem, and tigecycline against the *Mycobacterium abscessus* complex. *Antimicrob Agents Chemother* 63:e02234-18. <https://doi.org/10.1128/AAC.02234-18>.
 43. Luna-Herrera J, Reddy MV, Gangadharam PRJ. 1995. *In vitro* and intracellular activity of rifabutin on drug-susceptible and multiple drug-resistant (MDR) tubercle bacilli. *J Antimicrob Chemother* 36:355–363. <https://doi.org/10.1093/jac/36.2.355>.
 44. Bernut A, Le Moigne V, Lesne T, Lutfalla G, Herrmann J-L, Kremer L. 2014. *In vivo* assessment of drug efficacy against *Mycobacterium abscessus* using the embryonic zebrafish test system. *Antimicrob Agents Chemother* 58:4054–4063. <https://doi.org/10.1128/AAC.00142-14>.
 45. Dubée V, Bernut A, Cortes M, Lesne T, Dorcène D, Lefebvre A-L, Hugonnet J-E, Gutmann L, Mainardi J-L, Herrmann J-L, Gaillard J-L, Kremer L, Arthur M. 2015. β -Lactamase inhibition by avibactam in *Mycobacterium abscessus*. *J Antimicrob Chemother* 70:1051–1058. <https://doi.org/10.1093/jac/dku510>.
 46. Bernut A, Dupont C, Sahuquet A, Herrmann J-L, Lutfalla G, Kremer L. 2015. Deciphering and imaging pathogenesis and cording of *Mycobacterium abscessus* in zebrafish embryos. *J Vis Exp* 103:e53130. <https://doi.org/10.3791/53130>.
 47. Baysarowich J, Koteva K, Hughes DW, Ejim L, Griffiths E, Zhang K, Junop M, Wright GD. 2008. Rifamycin antibiotic resistance by ADP-ribosylation: structure and diversity of Arr. *Proc Natl Acad Sci U S A* 105:4886–4891. <https://doi.org/10.1073/pnas.0711939105>.
 48. Ganapathy US, Dartois V, Dick T. 2019. Repositioning rifamycins for *Mycobacterium abscessus* lung disease. *Expert Opin Drug Discov* 14:867–878. <https://doi.org/10.1080/17460441.2019.1629414>.
 49. Le Run E, Arthur M, Mainardi J-L. 2018. *In vitro* and intracellular activity of imipenem combined with rifabutin and avibactam against *Mycobacterium abscessus*. *Antimicrob Agents Chemother* 62:e00623-18. <https://doi.org/10.1128/AAC.00623-18>.
 50. Brambila C, Llorens-Fons M, Julián E, Noguera-Ortega E, Tomàs-Martínez C, Pérez-Trujillo M, Byrd TF, Alcaide F, Luquin M. 2016. Mycobacteria clumping increase their capacity to damage macrophages. *Front Microbiol* 7:1562. <https://doi.org/10.3389/fmicb.2016.01562>.
 51. Jagielski T, Bakula Z, Brzostek A, Minias A, Stachowiak R, Kalita J, Napiórkowska A, Augustynowicz-Kopec E, Zaczek A, Vasiliauskienė E, Bielecki J, Dziadek J. 2018. Characterization of mutations conferring resistance to rifampin in *Mycobacterium tuberculosis* clinical strains. *Antimicrob Agents Chemother* 62:e01093-18. <https://doi.org/10.1128/AAC.01093-18>.
 52. Richard M, Gutiérrez AV, Viljoen AJ, Ghigo E, Blaise M, Kremer L. 2018. Mechanistic and structural insights into the unique TetR-dependent regulation of a drug efflux pump in *Mycobacterium abscessus*. *Front Microbiol* 9:649. <https://doi.org/10.3389/fmicb.2018.00649>.
 53. Richard M, Gutiérrez AV, Viljoen A, Rodriguez-Rincon D, Roquet-Baneres F, Blaise M, Everall I, Parkhill J, Floto RA, Kremer L. 2018. Mutations in the MAB_2299c TetR regulator confer cross-resistance to clofazimine and bedaquiline in *Mycobacterium abscessus*. *Antimicrob Agents Chemother* 63:e01316-18. <https://doi.org/10.1128/AAC.01316-18>.
 54. Gutiérrez AV, Richard M, Roquet-Banères F, Viljoen A, Kremer L. 2019. The TetR-family transcription factor MAB_2299c regulates the expression of two distinct MmpS-MmpL efflux pumps involved in cross-resistance to clofazimine and bedaquiline in *Mycobacterium abscessus*. *Antimicrob Agents Chemother* 63:e01000-19. <https://doi.org/10.1128/AAC.01000-19>.
 55. Koteva K, Cox G, Kelso JK, Surette MD, Zubyk HL, Ejim L, Stogios P, Savchenko A, Sørensen D, Wright GD. 2018. Rox, a rifamycin resistance enzyme with an unprecedented mechanism of action. *Cell Chem Biol* 25:403–412.e5. <https://doi.org/10.1016/j.chembiol.2018.01.009>.
 56. Lefebvre A-L, Le Moigne V, Bernut A, Veckerlé C, Compain F, Herrmann J-L, Kremer L, Arthur M, Mainardi J-L. 2017. Inhibition of the β -lactamase BlaMab by avibactam improves the *in vitro* and *in vivo* efficacy of

- imipenem against *Mycobacterium abscessus*. Antimicrob Agents Chemother 61:e02440-16. <https://doi.org/10.1128/AAC.02440-16>.
57. Marshall VP, Cialdella JJ, Ohlmann GM, Gray GD. 1983. MIC values do not predict the intraphagocytic killing of *Staphylococcus aureus* by naphthalenic ansamycins. J Antibiot (Tokyo) 36:1549–1560. <https://doi.org/10.7164/antibiotics.36.1549>.
58. Viljoen A, Viela F, Kremer L, Dufrène YF. 2020. Fast chemical force microscopy demonstrates that glycopeptidolipids define nanodomains of varying hydrophobicity on mycobacteria. Nanoscale Horiz 5:944–953. <https://doi.org/10.1039/c9nh00736a>.
59. Halloum I, Carrère-Kremer S, Blaise M, Viljoen A, Bernut A, Le Moigne V, Vilchêze C, Guérardel Y, Lutfalla G, Herrmann J-L, Jacobs WR, Kremer L. 2016. Deletion of a dehydratase important for intracellular growth and cording renders rough *Mycobacterium abscessus* avirulent. Proc Natl Acad Sci U S A 113:E4228–E4237. <https://doi.org/10.1073/pnas.1605477113>.
60. Maurer FP, Bruderer VL, Ritter C, Castelberg C, Bloemberg GV, Böttger EC. 2014. Lack of antimicrobial bactericidal activity in *Mycobacterium abscessus*. Antimicrob Agents Chemother 58:3828–3836. <https://doi.org/10.1128/AAC.02448-14>.
61. Lee H, Ahn S, Hwang NY, Jeon K, Kwon OJ, Huh HJ, Lee NY, Koh W-J. 2017. Treatment outcomes of rifabutin-containing regimens for rifabutin-sensitive multidrug-resistant pulmonary tuberculosis. Int J Infect Dis 65:135–141. <https://doi.org/10.1016/j.ijid.2017.10.013>.
62. Griffith DE. 2018. Treatment of *Mycobacterium avium* complex (MAC). Semin Respir Crit Care Med 39:351–361. <https://doi.org/10.1055/s-0038-1660472>.
63. Blaschke TF, Skinner MH. 1996. The clinical pharmacokinetics of rifabutin. Clin Infect Dis 22(Suppl 1):S15–S21. discussion S21-22. https://doi.org/10.1093/clinids/22.Supplement_1.S15.
64. Le Run E, Arthur M, Mainardi J-L. 2019. In vitro and intracellular activity of imipenem combined with tedizolid, rifabutin, and avibactam against *Mycobacterium abscessus*. Antimicrob Agents Chemother 63:e01915-18. <https://doi.org/10.1128/AAC.01915-18>.
65. Singh S, Bouzinbi N, Chaturvedi V, Godreuil S, Kremer L. 2014. In vitro evaluation of a new drug combination against clinical isolates belonging to the *Mycobacterium abscessus* complex. Clin Microbiol Infect 20:O1124–O1127. <https://doi.org/10.1111/1469-0691.12780>.
66. Halloum I, Viljoen A, Khanna V, Craig D, Bouchier C, Brosch R, Coxon G, Kremer L. 2017. Resistance to thiacetazone derivatives active against *Mycobacterium abscessus* involves mutations in the MmpL5 transcriptional repressor MAB_4384. Antimicrob Agents Chemother 61:e02509-16. <https://doi.org/10.1128/AAC.02509-16>.
67. Woods GL, Brown-Elliott BA, Conville PS, Desmond EP, Hall GS, Lin G, Pfyffer GE, Ridderhof JC, Siddiqi SH, Wallace RJ. 2011. Susceptibility testing of mycobacteria, nocardiae and other aerobic actinomycetes: approved standard, 2nd ed. M24-A2. Clinical and Laboratory Standards Institute, Wayne, PA.
68. Lamason RL, Mohideen M-APK, Mest JR, Wong AC, Norton HL, Aros MC, Jurynek MJ, Mao X, Humphreville VR, Humbert JE, Sinha S, Moore JL, Jagadeeswaran P, Zhao W, Ning G, Makalowska I, McKeigue PM, O'donnell D, Kittles R, Parra EJ, Mangini NJ, Grunwald DJ, Shriver MD, Canfield VA, Cheng KC. 2005. SLC24A5, a putative cation exchanger, affects pigmentation in zebrafish and humans. Science 310:1782–1786. <https://doi.org/10.1126/science.1116238>.